No evidence for the cold spot in the NVSS radio survey

Kendrick M. Smith[1]★ and Dragan Huterer[2]

[1]*Institute of Astronomy, Cambridge University, Madingley Road, Cambridge CB3 0HA*
[2]*Department of Physics, University of Michigan, 450 Church St, Ann Arbor MI 48109, USA*

ABSTRACT

We revisit recent claims that there is a 'cold spot' in both number counts and brightness of radio sources in the NRAO (National Radio Astronomy Observatory) VLA (Very Large Array) Sky Survey (NVSS), with location coincident with the previously detected cold spot in *Wilkinson Microwave Anisotropy Probe*. Such matching cold spots would be difficult if not impossible to explain in the standard Λcold dark matter cosmological model. Contrary to the claim, we find no significant evidence for the radio cold spot, after including systematic effects in NVSS, and carefully accounting for the effect of a posteriori choices when assessing statistical significance.

Key words: cosmic microwave background – large-scale structure of Universe.

1 INTRODUCTION

Cosmic microwave background (CMB) maps have been studied in detail during the last few years. These studies have been motivated by the remarkable full-sky high-resolution maps obtained by *Wilkinson Microwave Anisotropy Probe (WMAP)* (Bennett et al. 2003; Spergel et al. 2007), and led to a variety of interesting and unexpected findings. Notably, various anomalies have been claimed pertaining to the alignment of largest modes in the CMB (Hajian & Souradeep 2003; Tegmark, de Oliveira-Costa & Hamilton 2003; de Oliveira-Costa et al. 2004; Schwarz et al. 2004; Slosar & Seljak 2004; Land & Magueijo 2005a,b; Copi, Huterer, Schwarz & Starkman 2006), the missing power on large angular scales (Spergel et al. 2003; Copi et al. 2007) and the asymmetries in the distribution of power (Eriksen et al. 2004; Bernui et al. 2006; Hajian 2007). In the future, temperature maps obtained by the Planck experiment and large-scale polarization information (Dvorkin, Peiris & Hu 2008) may be key to determining the nature of the large-scale anomalies. For a review of the anomalies and attempts to explain them, see Huterer (2006).

Recently, a paper by Rudnick, Brown & Williams (2007) attracted particular attention, as it claimed to have detected a 'cold spot' – a drop in the source density *and* brightness in the NRAO VLA Sky Survey (NVSS). This claim would be relatively unremarkable, if it were not for the fact that a previously reported, anomalously cold spot in the *WMAP* microwave signal (Vielva et al. 2004; Cayón, Jin & Treaster 2005; Cruz et al. 2005, 2006, 2007) apparently lies at roughly the same location.

This claim, if verified to be true at high statistical significance, would represent a major result, and would be difficult or impossible to explain in the standard cosmological model. One interpretation, proposed in Inoue & Silk (2006) and Rudnick et al. (2007), is

the existence of a large ($\gtrsim$100 Mpc) void at $z \sim 1$, which gives rise to an NVSS underdensity directly and to the *WMAP* cold spot via the non-linear Integrated Sachs–Wolfe (ISW) effect. However, the probability of forming such a large void in Λcold dark matter cosmology is negligibly small.

Here, we re-examine these claims using our own analysis procedure, carefully including known systematic and statistical properties of NVSS (declination-dependent 'striping' and galaxy–galaxy correlations; see Section 3.1), and marginalizing a posteriori choices when assessing statistical significance. We will argue that there is no statistically significant evidence for either a dip in NVSS number counts or median source flux in the *WMAP* cold spot. We will see that it is possible to construct statistics containing a posteriori choices (e.g. the location and radius of a 'subdisc' of the cold spot) which might appear to support an underdense region, but the statistical significance goes away when these choices are properly marginalized. Furthermore, we will show that by making different a posteriori choices, we could find evidence for an *overdense* region with the same statistical significance as an underdense region.

The paper is organized as follows. In Section 2, we describe the NVSS data and selection cuts that we consider. In Section 3, we perform statistical tests using the number density distribution of NVSS sources and in Section 4 we do the same for the flux distribution. In Section 5, we study the dependence of our results on the selection cuts that are applied to the NVSS catalogue prior to the analysis. Our main result, showing significance of anomalous number counts or source fluxes in the *WMAP* cold spot, using several different statistics and with a range of possible selection cuts in the NVSS catalogue, is shown in Table 1. We conclude in Section 6.

2 DATA

The NVSS is a 1.4 GHz continuum survey, covering 82 per cent of the sky, with a source catalogue containing over 1.8×10^6 sources that is 50 per cent complete at 2.5 mJy. Away from the galactic

★E-mail: kmsmith@ast.cam.ac.uk

Table 1. Statistical significance of anomalous NVSS number counts or median flux in the *WMAP* cold spot, for different NVSS flux ranges, and with complex sources either dropped (unparenthesized values) or retained (parenthesized) in the analysis. The six columns correspond to the different number count and median flux analyses that we have considered in Sections 3–4. As described in Section 5, each entry in the table is either the statistical significance of a region with high source density/flux (positive sign), or low source density/flux (negative sign), depending on which has higher significance. An entry is marked '–' if we do not find any subdisc (either overdense or underdense) which is more anomalous than expected from statistics. (This is assessed by comparing to an ensemble of regions with the same size and declination as the cold spot, as explained in detail in Section 5.) As described in the text, the NVSS source density is roughly 46 deg^{-2}, the flux ranges chosen in the table roughly divide the catalogue into quartiles, and the discs used in the analysis have radii in the range $1 \le r \le 5$ deg. Thus the discs used to construct the table contain between ≈ 36 and ≈ 3600 sources.

Flux range	NVSS galaxy counts analysis			NVSS median flux analysis		
	WMAP centre *and* radius	*WMAP* centre, any radius	Any centre, any radius	*WMAP* centre *and* radius	*WMAP* centre, any radius	Any centre, any radius
$S \le 3$ mJy	-0.5σ (-0.5σ)	-0.8σ (-0.7σ)	– (-0.0σ)	0.1σ (0.2σ)	0.2σ (0.2σ)	– (–)
$3 \le S \le 5$ mJy	0.4σ (0.2σ)	– (–)	– (–)	1.1σ (0.9σ)	0.3σ (–)	2.5σ (-2.9σ)
$5 \le S \le 12$ mJy	2.6σ (2.3σ)	2.0σ (1.6σ)	1.7σ (1.7σ)	0.4σ (0.1σ)	-0.9σ (-0.9σ)	1.4σ (1.3σ)
$S \ge 12$ mJy	-0.4σ (-0.6σ)	– (-0.2σ)	-1.4σ (-1.6σ)	1.3σ (0.5σ)	-1.4σ (-1.2σ)	-1.6σ (-2.2σ)
$S \le 5$ mJy	-0.2σ (-0.3σ)	-0.5σ (-0.6σ)	– (-0.1σ)	0.8σ (0.8σ)	0.1σ (0.1σ)	0.3σ (0.2σ)
$S \ge 5$ mJy	1.4σ (1.0σ)	0.6σ (-0.2σ)	-1.8σ (-2.5σ)	-1.7σ (-1.7σ)	-1.1σ (-1.0σ)	-1.6σ (-2.0σ)
Arbitrary S	0.9σ (0.5σ)	-0.1σ (-0.6σ)	-0.9σ (-1.2σ)	0.7σ (0.5σ)	0.4σ (0.2σ)	-0.6σ (-0.8σ)

plane, almost all of the sources are extragalactic: quasars or active galactic nuclei powered or star-forming galaxies. The NVSS catalogue covers a wide range of redshifts (the median redshift is $z \approx 0.9$), but dividing the catalogue into redshift bins is not possible because per-source redshifts are not measured. However, in Section 5 we will explore the effect of dividing the catalogue into flux bins.

When making Healpix (Gorski et al. 2005) maps from the NVSS catalogue, we mask pixels near the galactic plane ($|b| < 10°$) or the boundary of the survey (declination $\delta < -37°$). Our 'default cuts' will consist of this pixel mask plus dropping all sources which are flagged in the NVSS catalogue as having complex structure. (These are mainly galactic sources; if they are included in the maps then spurious features can be seen by eye at low galactic latitude.) We will also consider other choices of cuts in Section 5.

In Fig. 1, we show a full-sky map and a zoomed-in region near the *WMAP* cold spot, with default selection cuts and smoothed to $1°$ resolution. We have shown the full-sky map in equatorial coordinates to highlight a known systematic effect in NVSS (Blake & Wall 2002): the presence of declination-dependent variations in completeness level, most notably the underdense 'stripe' at $\delta \lesssim -10°$. Because the *WMAP* cold spot is inside the stripe, modelling these variations will play an important role in the analysis, as we will see in detail below.

3 GALAXY COUNT ANALYSIS

In Cruz et al. (2005), the *WMAP* cold spot is given as a circular region with centre P_0 at $(l, b) = (209°, -57°)$ in galactic coordinates and radius $r_0 = 5°$. However, in Rudnick et al. (2007) the most anomalously underdense circular region in NVSS is quoted as having centre P_0' at $(l, b) = (207.03, -54.85)$ and radius $r_0' = 1°$. How does this mismatch between the *WMAP* cold spot and the NVSS underdense region affects the analysis? The total statistical significance of the *WMAP* cold spot is only $\approx 3\sigma$. Presumably, at this significance, the best-fitting centre and radius have non-negligible statistical errors, and any non-trivial shape or substructure of the cold spot is not resolved.

For this reason, it seems reasonable to look for an NVSS underdensity (P_0', r_0') which need not be equal to the *WMAP* cold spot $(P_0,$
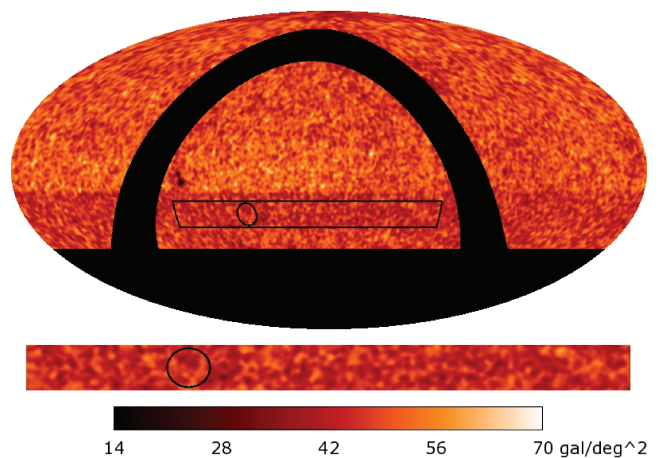

Figure 1. Galaxy count maps for the NVSS, smoothed to $1°$ radius and plotted in equatorial coordinates, with default data cuts as described in Section 2. The full-sky counts (top panel) show declination-dependent variations in completeness level; the *WMAP* cold spot (shown as a circle in both panels) is entirely contained within the underdense 'stripe' at declination $\delta \lesssim -10°$. If we zoom in on a box at the same declination as the cold spot, then the *WMAP* cold spot does not look anomalous by eye (bottom panel; shown as a rectangular region in the top panel).

r_0). However, this makes statistical significance more difficult to assess: for a correct treatment, the parameters (P_0', r_0') must be treated as a posteriori choices. Alternately, one could simply ask whether the region (P_0, r_0) is underdense in NVSS. In this case, there are no a posteriori choices (we are simply counting NVSS galaxies using the best-fitting cold-spot parameters from *WMAP* data alone) and computing statistical significance is straightforward.

Our perspective is that either of these analyses is valid; in the next three sections we consider the following possibilities for a disc-shaped NVSS underdensity with centre P and radius r:

(1) $P = P_0, r = r_0$: the NVSS underdensity has the same centre and radius as the *WMAP* cold spot.

(2) $P = P_0, r \ne r_0$: the NVSS underdensity has the same centre as the *WMAP* cold spot but its radius is different; then we must

assign statistical significance in a way which incorporates the a posteriori choice of radius.

(3) $P \subseteq P_0, r \neq r_0$: the NVSS underdensity lies wholly within the *WMAP* cold spot but both its centre and its radius are different; then we must incorporate the a posteriori choice of both radius and location.

3.1 Case 1: fixed centre, fixed radius

This case ($P = P_0, r = r_0$) corresponds to the simplest possible question: if we count the total number of galaxies in the *WMAP* cold spot, do we get an anomalous value? We introduce the ratio statistic

$$\frac{N_{\mathrm{gal}}(P_0, r_0)}{\langle N_{\mathrm{gal}}(P_0, r_0)\rangle} \tag{1}$$

and ask whether it differs from 1.0 with statistical significance, where the numerator $N_{\mathrm{gal}}(P_0, r_0)$ denotes the number of galaxies in the *WMAP* cold spot (P_0, r_0) and the denominator is its expectation value.

Two issues arise here: first, how should the denominator $\langle N_{\mathrm{gal}}(P_0, r_0)\rangle$ be computed? The simplest prescription would be to assume that the expected number density per unit area is equal to the full-sky NVSS average:

$$\langle N_{\mathrm{gal}}(P, r)\rangle = \pi r^2 \langle n\rangle_{\mathrm{full-sky}}, \tag{2}$$

where $\langle n\rangle_{\mathrm{full-sky}}$ is the mean number density per unit area on the full NVSS sky. This simple estimate for $\langle N_{\mathrm{gal}}\rangle$ is not satisfactory because it does not account for the underdense stripe (see Fig. 1). Therefore, we also consider an improved prescription based on a simple stripe model. We assume that the expected number of galaxies in each Healpix pixel p is equal to the average taken over unmasked pixels p' at the same declination:

$$\langle N_{\mathrm{gal}}(P, r)\rangle = \sum_{p \in (P, r)} \langle N_{\mathrm{gal}}(p')\rangle_{p' \sim p}, \tag{3}$$

where the sum runs over pixels p in the disc (P, r), and $\langle N_{\mathrm{gal}}(p')\rangle_{p' \sim p}$ denotes the average galaxy count taken in pixels p' at the same declination as p.

The second issue when studying the ratio statistic in equation (1) is how error bars should be assigned. Here, the simplest prescription would be to assume Poisson statistics: we take the uncertainty in the numerator to be given by

$$\Delta N_{\mathrm{gal}}(P, r) = \langle N_{\mathrm{gal}}(P, r)\rangle^{1/2}. \tag{4}$$

This simple prescription for $\langle \Delta N_{\mathrm{gal}}\rangle$ underestimates the error bars because it assumes that the NVSS galaxies are pure shot noise, i.e. galaxy–galaxy correlations are ignored.[1] Therefore, we also consider an improved prescription: we estimate $\langle \Delta N_{\mathrm{gal}}\rangle$ directly from the data by taking the rms fluctuation over alternate choices P' of ring centre which lie at the same declination as P:

$$\frac{\Delta N_{\mathrm{gal}}(P, r)}{\langle N_{\mathrm{gal}}(P, r)\rangle^{1/2}} = \mathrm{rms}_{P' \sim P}\left[\frac{N_{\mathrm{gal}}(P', r) - \langle N_{\mathrm{gal}}(P', r)\rangle}{\langle N_{\mathrm{gal}}(P', r)\rangle^{1/2}}\right], \tag{5}$$

where the notation $\mathrm{rms}_{P' \sim P}(\cdot)$ denotes the rms fluctuation taken over choices of centre P' with the same declination as P.[2]

With default cuts (Section 2), we find the following results. If we use full-sky averaging (equation 2) and Poisson errors (equation 4), then the *WMAP* cold spot appears to be underdense in NVSS sources at 3.1σ. However, this is simply an artefact of using the full-sky average galaxy density when computing $\langle N_{\mathrm{gal}}\rangle$; in fact, the *WMAP* cold spot is contained within the underdense NVSS stripe (Fig. 1). If we improve the estimate of $\langle N_{\mathrm{gal}}\rangle$ by using isolatitude averaging (equation 3) then the cold spot appears *overdense* at 1.1σ. This is already not statistically significant, but if we improve the estimate of $\Delta N_{\mathrm{gal}}(P, r)$ using equation (5), then the overdensity drops to 0.8σ. We conclude that the *WMAP* cold spot, taken as a whole, is not underdense or overdense in NVSS sources, but modelling the NVSS 'stripe' plays a crucial role in the analysis.

We note that declination-dependent striping is unlikely to affect the analysis of Rudnick et al. (2007), which is restricted to small regions of sky near the cold spot. The discussion here is intended to motivate expressions such as $\langle \Delta N_{\mathrm{gal}}\rangle$ above (equation 3), and related quantities later in the paper, which are defined in a way which is robust to striping.

3.2 Case 2: fixed centre, floating radius

We next consider the possibility of an underdense region with the same centre $P = P_0$ as the *WMAP* cold spot but arbitrary radius $r < r_0$. We again define a ratio statistic

$$\frac{N_{\mathrm{gal}}(P_0, r)}{\langle N_{\mathrm{gal}}(P_0, r)\rangle} \tag{6}$$

and compute the expectation value $\langle N_{\mathrm{gal}}(P_0, r)\rangle$ and rms deviation $\Delta N_{\mathrm{gal}}(P_0, r)$ following the discussion in the preceding subsection.

Results using this statistic are shown (with default cuts) in Fig. 2. The rightmost error bars represent our most accurate ways of computing $\langle N_{\mathrm{gal}}\rangle$ and $\langle \Delta N_{\mathrm{gal}}\rangle$ (equations 3 and 5); we find that all points are within 1σ of the expected level, i.e. no evidence for an underdensity is seen. (We note that if, say, one value of r gave an anomalous value, then we would have to incorporate the a posteriori choice of r when assessing significance; we revisit this issue in Section 5.) The left and middle error bars represent less accurate ways of computing $\langle N_{\mathrm{gal}}\rangle$ and $\langle \Delta N_{\mathrm{gal}}\rangle$ (equations 2 and 4) and are shown for comparison.

3.3 Case 3: floating centre, floating radius

The result of the preceding section appears to contradict fig. 5 in Rudnick et al. (2007), where a statistically significant underdense disc of radius $r_0' = 1°$ is seen. However, this figure has been constructed taking the disc centre P_0' to be the point $(l, b) = (207.03, -54.85)$ rather than the centre P_0 of the *WMAP* cold spot which is at $(l, b) = (209, -57)$.

If the choice of (P_0', r_0') had an a priori motivation, then we would find, using an analysis similar to Section 3.1, a 2.0σ underdensity, with our default cuts. [There are other underdense 'subdiscs' as well, e.g. we find that the subdisc centred at $(l, b) = (206.82, -56.4)$ with radius $2°.5$ is underdense at 3.06σ if a posteriori choices are

---

[1] In principle, this could be remedied by estimating the galaxy power spectrum and including it in Monte Carlo simulations, although this may be difficult in practice, due to the presence of long-wavelength instrumental power in NVSS at low flux levels (Smith, Zahn & Doré 2007; Ho et al. 2008) which may not be accurately modelled by an isotropic Gaussian field. In equation (5), we have taken a simpler approach by averaging over choices of disc centre P' in the real NVSS data, rather than averaging over Monte Carlo simulations.

[2] As a minor point, in equation (5) we have normalized each value of N_{gal} by its Poisson error $\langle N_{\mathrm{gal}}\rangle^{1/2}$ before taking the rms; this slightly improves the estimate of $\langle \Delta N_{\mathrm{gal}}\rangle$ by accounting for variations in $\langle N_{\mathrm{gal}}\rangle$ due to striping and the pixel mask.
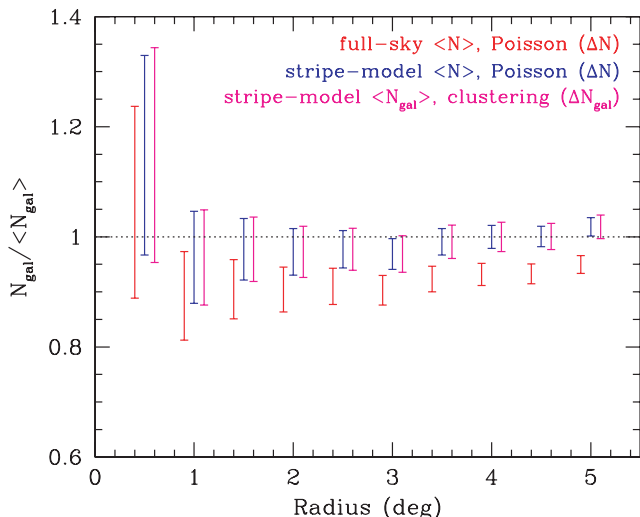
Figure 2. Galaxy counts in circles of varying radii centred at the *WMAP* cold-spot location, relative to expected counts as in equation (1). From left to right, the three sets of error bars (all 68 per cent CL) represent increasingly accurate analysis methods. The left error bars assume full-sky $\langle N_{gal}\rangle$ and Poisson (ΔN_{gal}) (equations 2 and 4). The middle and right error bars incorporate declination striping in $\langle N_{gal}\rangle$ and galaxy–galaxy clustering in (ΔN_{gal}), respectively (equations 3 and 5). It is seen that if the NVSS underdense stripe is not modelled, then the *WMAP* cold spot appears to be anomalously underdense, but the statistical significance is lost when the stripe is included in the analysis.

ignored.] However, we see no a priori motivation for making such choices of (P'_0, r'_0), and we must therefore incorporate the effect of the a posteriori choice when calculating statistical significance.

To assess significance fairly, we incorporate the effect of the choice of (P'_0, r'_0) as follows. Formally, given a disc (P, r), define the 'naive number of sigmas' of its worst underdense subdisc by

$$N_\sigma(P, r) = \min_{(P',r')\subset(P,r)} \left[\frac{N_{gal}(P', r') - \langle N_{gal}(P', r')\rangle}{\Delta N_{gal}(P', r')} \right], \quad (7)$$

where the notation $\min_{(P',r')\subset(P,r)}(\cdot)$ means that the quantity in parentheses is minimized over discs (P', r') which are entirely contained in (P, r), with minimum radius $r'_{min} = 1°$. In this notation, the existence of the 'subdisc' (P'_0, r'_0) from the preceding paragraph can be rephrased as the statement that $N_\sigma(P_0, r_0) = -3.06$, where (P_0, r_0) are the cold-spot centre and radius, respectively.

To assess whether this value is anomalous, we evaluate the same statistic ('number of sigmas of the worst underdense subdisc') in an ensemble of disc-shaped regions with the same size and declination as the *WMAP* cold spot. This way of assessing significance accounts for both the a posteriori choice of (P'_0, r'_0) and declination-dependent striping. More precisely, we compute $N_\sigma(P, r_0)$ for an ensemble of alternate choices of disc centre P with the same declination as the *WMAP* cold-spot centre P_0 and with radius $r_0 = 5°$. We find that this ensemble of values has mean $\langle N_\sigma\rangle = -2.65$ and rms error $(\Delta N_\sigma) = 0.45$. Therefore, the cold spot (with $N_\sigma = -3.06$) is typical among discs with the same radius and declination, and the 'subdisc' described above does not have statistical significance after the effect of a posteriori choices is taken into account.

4 FLUX ANALYSIS

In addition to number counts, the median NVSS brightness was also reported to be low near the *WMAP* cold spot in Rudnick et al.
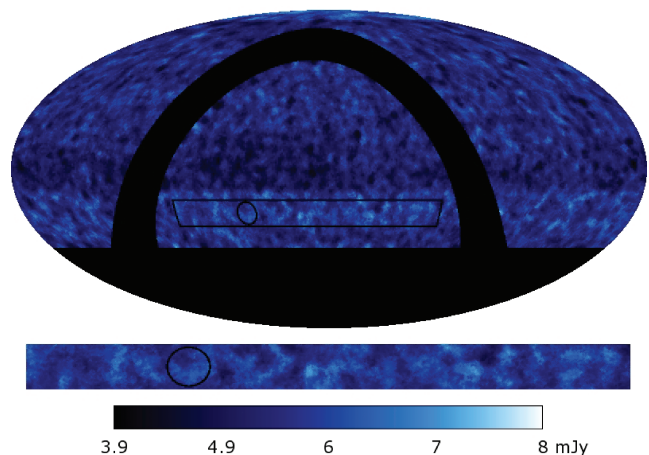

Figure 3. NVSS flux maps, smoothed by 2° median filtering as described in Section 4, shown with default cuts in equatorial coordinates. As in the galaxy-count case (Fig. 1), the full-sky map (top panel) shows declination-dependent variations in median flux, and the *WMAP* cold spot (shown as a circle) is not anomalous by eye when viewed in a 'box' at the same declination (bottom panel).

(2007). Since brightness is roughly proportional to (source counts) × (source flux), and we have already analysed the source counts, our perspective is that it is better to separate the two issues and next ask whether median source fluxes in NVSS are anomalous in the *WMAP* cold spot. Considering source counts and fluxes separately, rather than using brightness maps, has two additional advantages. First, it allows the analysis to proceed from the NVSS source catalogue, thus avoiding instrumental complexities associated with working with the NVSS images, which have been incorporated by the NVSS team when constructing the source catalogue. Secondly, it avoids introducing more a posteriori choices which must be marginalized [e.g. in Rudnick et al. (2007), the brightness maps are convolved with an 800 arcsec filter to obtain a continuous field, which is then median filtered in sliding boxes with side length 3°.4; a 'dip' is then observed at a point other than the *WMAP* cold-spot centre].

We would also like to emphasize that if the purpose of this analysis is to find voids, then there is no a priori motivation for considering either brightness or source fluxes; the best-motivated statistics would be based on number counts alone. Nevertheless, in this section, we will briefly discuss NVSS source fluxes in the *WMAP* cold spot. Our median flux analysis will be analogous to the galaxy-count case from the preceding section; we summarize our methodology and results here.

In Fig. 3, we show a flux map obtained by taking the median flux of all NVSS sources within 2° of each pixel. This median-based smoothing procedure was used because the NVSS flux distribution contains far outliers; if the mean were used instead of the median, then the map would be dominated by a small number of rare bright sources. Note that declination-dependent striping is seen in the flux map, as seen previously for number counts (Fig. 1).

Given disc centre P and radius r, we define $\mu(P, r)$ to be the median flux of all NVSS galaxies contained in the disc (P, r), and consider ratio statistics of the form

$$\frac{\mu(P, r)}{\langle\mu(P, r)\rangle}. \quad (8)$$

We estimate the expected median flux $\langle\mu(P, r)\rangle$ directly from the data by averaging over alternate choices of centre P' with the same

declination as P:

$$\langle \mu(P, r) \rangle = \langle \mu(P', r) \rangle_{P' \sim P}. \tag{9}$$

We also estimate the error $(\Delta\mu(P, r))$ from the data in an analogous way[3]

$$\Delta\mu(P, r) = \frac{\mathrm{rms}_{P' \sim P} \langle N_{\mathrm{gal}}(P', r) \rangle^{1/2} (\mu(P', r) - \langle \mu(P', r) \rangle)}{\langle N_{\mathrm{gal}}(P, r) \rangle^{1/2}}. \tag{10}$$

We then consider three cases for the disc (P, r), as in Sections 3.1–3.3.

(1) Fixed centre, fixed radius $(P = P_0, r = r_0)$: in this case, we simply evaluate the ratio statistic in equation (8), taking (P, r) to be the *WMAP* cold-spot centre and radius (P_0, r_0). We find that the ratio exceeds 1.0 by 0.6σ, i.e. the median flux of all NVSS galaxies in the *WMAP* cold spot is not anomalous.

(2) Fixed centre, floating radius $(P = P_0, r < r_0)$: in this case, we compute the ratio statistic in equation (8) for a variety of radii centred at the cold-spot centre P_0 (in analogy with Fig. 2). We find that all values are within 1.2σ of 1.0, i.e. no anomalous value of the median flux is found.

(3) Floating centre, floating radius $(P \subseteq P_0, r < r_0)$: in this case, we choose a subdisc (P, r) of the *WMAP* cold spot (P_0, r_0) which appears to give the most anomalous value of the ratio statistic in equation (8). If we look for an anomalously low median flux, then we find that the subdisc with centre $(l, b) = (206.81, -54.75)$ and radius $1°$ appears to be low at 2.2σ, if a posteriori choice of (P, r) is temporarily ignored. To assess whether this value is really anomalous, we proceed in parallel with the number count analysis in Section 3.3: we evaluate the same statistic (naive 'number of sigmas' N_σ of the most anomalous subdisc') over an ensemble of regions with the same size and declination as the cold spot. We get $N_\sigma = (2.2 \pm 0.3)$ in this ensemble, i.e. the *WMAP* cold spot (with $N_\sigma = 2.2$) is a typical member of this ensemble, and the low flux in the aforementioned subdisc has no statistical significance.

5   ALTERNATE CHOICES OF CUTS

We have now performed an exhaustive analysis of NVSS number density (Section 3) and median flux (Section 4) in subspots of the *WMAP* cold spot, with three cases depending on whether the subspot location and radius are determined a priori or a posteriori, for a total of six analyses in all. This has been done using our 'default cuts' from Section 2: we drop NVSS sources flagged as having complex structure to be conservative, but do not impose flux cuts, in order to avoid making an a posteriori choice of flux range.

One possible loophole remains: in fig. 5 in Rudnick et al. (2007), the statistical significance appears to be much higher if only sources with flux $S \geq 5$ mJy are retained. In this section, we consider the general question: can we get a statistically significant result if we use selection cuts other than our default choice? We divide the NVSS catalogue into four flux bins, with delimiting values given by {3, 5, 12} mJy. We also consider either dropping or retaining sources flagged as having complex structure in the NVSS catalogue. For reference, the source density of NVSS is 46 deg^{-2} with complex sources dropped, or 49 deg^{-2} with complex sources retained. The

delimiting values for our four flux bins were chosen to further divide the catalogue into quartiles.

In Table 1, we summarize the results of repeating the six analyses considered in this paper with various sets of cuts. This table presents many results in compressed form and is organized as we now explain.

Columns labelled 'fixed centre, fixed radius' correspond to Case 1 in Sections 3–4: we simply compute the total number (or median flux) of galaxies inside the *WMAP* cold spot, and report the deviation (in 'sigmas') from the expected value. A positive sign indicates a result (either count or flux) which is larger than expected; a negative sign indicates a result which is less than the expected value.

Columns in Table 1 labelled 'floating centre, floating radius' correspond to Case 3 in Sections 3–4. Each entry in these columns corresponds to a complete analysis along the lines of Section 3.3 and has been calculated as follows:

We first compute the statistic $N_\sigma(P_0, r_0)$, defined in equation (7) to measure the 'number of sigmas' of the worst underdense subdisc of the *WMAP* cold spot (P_0, r_0). As explained in Section 3.3, this statistic cannot be used directly to assess significance since the subdisc is an a posteriori choice. We therefore define

$$\mathcal{N}_{\mathrm{under}} = \frac{N_\sigma(P_0, r_0) - \langle N_\sigma \rangle}{\Delta N_\sigma}, \tag{11}$$

where $\langle N_\sigma \rangle$ and (ΔN_σ) are the mean and rms of the quantity $N_\sigma(P_0, r_0)$ taken over an ensemble of regions with the same size and declination as the cold spot. For example, with default cuts, the analysis in Section 3.3 can be summarized by the statement that $N_\sigma(P_0, r_0) = -3.06$ and $\mathcal{N}_{\mathrm{under}} = (-3.06 + 2.65)/0.45 = -0.9$. The interpretation is that the 'floating centre, floating radius' analysis has found an underdense subdisc of the cold spot with significance 0.9σ.

The sign convention in equation (11) has been chosen so that a negative value of $\mathcal{N}_{\mathrm{under}}$ corresponds to an underdensity which is more anomalous than the ensemble mean. A positive sign would mean that the most underdense subdisc in the *WMAP* cold spot is less anomalous than expected, when compared to an ensemble of regions with the same size and declination as the cold spot.

We define a quantity $\mathcal{N}_{\mathrm{over}}$ in an analogous way, choosing the sign so that a positive value corresponds to an overdense region which is more anomalous than the ensemble mean.

In Table 1, we report either $\mathcal{N}_{\mathrm{under}}$ (indicated by a negative sign) or $\mathcal{N}_{\mathrm{over}}$ (indicated by a positive sign), *whichever is more anomalous*. A '—' entry means that $\mathcal{N}_{\mathrm{under}}$ is positive and $\mathcal{N}_{\mathrm{over}}$ is negative, i.e. we find no subdisc (either underdense or overdense) of the cold spot which is more anomalous than the ensemble mean, for a given set of cuts.

For example, with default cuts, we find a negative value for $\mathcal{N}_{\mathrm{over}}$, i.e. the most anomalously overdense subdisc of the *WMAP* cold spot is actually less overdense than the ensemble mean. Therefore, the corresponding entry in Table 1 is given by $\mathcal{N}_{\mathrm{under}} = -0.9$. This value summarizes the analysis from Section 3.3: with default cuts, we find a subdisc which is anomalously underdense at 0.9σ (and any overdense subdisc is less anomalous than this).

Finally, columns in Table 1 labelled 'fixed centre, floating radius' correspond to Case 2 from Sections 3–4, with one difference: when reporting the significance of the most anomalous radius r, we incorporate the a posteriori choice of radius by maximizing over r as in Case 3. (We omitted this step for simplicity in Sections 3–4 because with our default cuts, all choices of r turned out to give very typical values.)

---

[3] Note that we have taken the factor $\langle N_{\mathrm{gal}} \rangle^{1/2}$ inside the rms average to improve the estimate of $(\Delta\mu)$ by accounting for the scaling $(\Delta\mu \propto N_{\mathrm{gal}}^{-1/2})$ expected due to variations in number density alone.

There are a few values in Table 1 which might be interpreted as statistically significant, e.g. the example which motivated this section: for the flux range $S \geq 5$ mJy, there is a subdisc (the 'floating centre, floating radius' case) which has galaxy counts low at 2.5σ even after accounting for the a posteriori choice of centre and radius. However, we note that the statistical significance goes away when complex sources are dropped, or if we restrict the flux range further. Furthermore, one can find another value in the table which supports an *overdensity* with the same statistical significance (the 'fixed centre, fixed radius' galaxy-count case with flux range $5 \leq S \leq 12$ mJy). Given the large number of entries in Table 1, a few high-significance values such as these are expected as statistical events.[4]

Analogously, for the flux analysis, there is a 2.9σ low-flux subdisc in the flux range $3 \leq S \leq 5$ mJy, but if complex sources are dropped, we find a 2.5σ *high-flux* disc in the same flux range. Since there is no clear pattern to the few high-significance values, and since a high source density/flux region is supported as well as a low source/flux region, our interpretation of Table 1 is that there is no evidence for either NVSS number counts or median source fluxes which are atypical in the *WMAP* cold spot.

6 DISCUSSION AND CONCLUSIONS

In this paper, we have revisited claims from Rudnick et al. (2007) that there is a cold spot in the NVSS radio survey which is statistically significant and aligned with the cold spot found in *WMAP* (Vielva et al. 2004; Cruz et al. 2005). We found no evidence for either an underdensity in NVSS number counts or a region of atypical median source flux.

Our analysis incorporates systematic declination-dependent striping in NVSS, by estimating quantities such as $\langle N_{\mathrm{gal}}(P, r) \rangle$ directly from the data via isolatitude averaging (e.g. equation 3). In an analogous way, we incorporate statistical clustering of galaxies in NVSS by estimating variances over isolatitude rings (e.g. equation 5).

Simple, direct statistical tests, such as counting the total number of all NVSS galaxies in the *WMAP* cold spot, or taking the median flux of all such galaxies, do not show any statistically significant anomaly. (This corresponds to Case 1 in Sections 3–4.) Things only become murky when one considers statistics with many a posteriori choices, such as anomalous subdisc of the cold spot (Case 3), or a choice of selection cuts which maximizes the quoted significance (Table 1). We have exhaustively studied many such statistical tests and argued that when the a posteriori choices are included in the assessment of statistical significance, there is no evidence for an NVSS 'cold spot'.

As a concrete example, consider the '$S \geq 5$ mJy' case in fig. 5 of Rudnick et al. (2007), which seems to show a $\approx 5\sigma$ underdense region, if the error bars are taken at face value. We agree with the number counts that are plotted in this figure, but disagree that there is statistically significant evidence for an underdensity. Let us illustrate this by following this example through the steps of this paper one at a time. First, if we use our most accurate prescriptions for the rms error (ΔN_{gal}) and the expected count $\langle N_{\mathrm{gal}} \rangle$

(equations 3 and 5), then we find that the statistical significance drops to 3.4σ; however this ignores the effect of a posteriori choices. The centre of this underdense region is not the *WMAP* cold-spot centre, and if we account for this choice (and the a posteriori choice of radius) using the method of Section 3.3, then we find that the significance decreases to 2.5σ.

This now accounts for the a posteriori choice of subdisc, and appears to give a statistically significant result, but we have still made an a posteriori choice of selection cuts, by allowing complex structure and considering only sources with flux $S \geq 5$ mJy. When viewed in the larger context of Table 1, it is seen that these choices maximize the quoted 'number of sigmas' of an underdensity, and simply reflect the large number of possible choices of selection cuts: the significance goes away if the cuts are changed slightly, and in fact a different choice of cuts would favour an *overdensity* rather than an underdensity, with roughly the same significance. This last observation is perhaps the most convincing sign that the apparent $\approx 2.5\sigma$ underdensity, for a single choice of selection cuts, is spurious.

For the median flux analysis (Section 4), our conclusions are the same: we find no evidence for atypical source fluxes in the *WMAP* cold spot, after accounting for a posteriori choices. There are a few choices of cuts which appear to show anomalous values (if the a posteriori choice of cuts is ignored), but the number of such values is consistent with statistics, and the cuts can be tuned to support either a region with high or low source density/flux with roughly the same statistical significance (Table 1).

We do not see reason to give preferential treatment to a posteriori choices in the analysis and selection cuts given in Rudnick et al. (2007), and we instead considered a range of analysed quantities and selection criteria. Had there been a physical reason or a survey-specific requirement for the particular treatment of raw data used in Rudnick et al. (2007), we would have agreed with that choice being well motivated or even necessary. However, since we do not see such motivation, we insist on calling all such choices a posteriori.

In McEwen et al. (2007), the cold spot was identified as one of 18 regions which are 'peaks' in the ISW cross-correlation between *WMAP* and NVSS. However, this analysis was performed using wavelet smoothing with scale 250 arcmin and would be blind to the $1°$ underdense region studied in Rudnick et al. (2007). Furthermore, it is not clear from the analysis in McEwen et al. (2007) whether the *WMAP*–NVSS cross-correlation is statistically significant when restricted to the cold spot alone.

Despite the null result of this paper, one should not be disheartened. More detailed observation of the cold-spot region in galaxy surveys will likely improve confidence about the existence of any over-/underdensity or lack thereof. More generally, new *WMAP* data and the eagerly expected Planck maps expected in a few years, combined with data from a variety of galaxy surveys from ground and space, will provide a gold mine to search for signatures of the early- and late-universe physics in the large-scale structure and the CMB.

---

[4] To make this more quantitative, given only four independent events, the likelihood that one event is anomalous at the 2.5σ level is $\approx 2\sigma$, so getting a few such anomalous values in an analysis such as Table 1 with many different choices of cuts is not surprising.

REFERENCES

Bennett C. L. et al., 2003, ApJS, 148, 1

Bernui A., Villela T., Wuensche C. A., Leonardi R., Ferreira I., 2006, A&A, 454, 409

Blake C., Wall J., 2002, MNRAS, 329, L37

Cayón L., Jin J., Treaster A., 2005, MNRAS, 362, 826

Copi C. J., Huterer D., Schwarz D. J., Starkman G. D., 2006, MNRAS, 367, 79

Copi C. J., Huterer D., Schwarz D. J., Starkman G. D., 2007, Phys. Rev. D, 75, 023507

Cruz M., Martinez-Gonzalez E., Vielva P., Cayón L., 2005, MNRAS, 356, 29

Cruz M., Tucci M., Martinez-Gonzalez E., Vielva P., 2006, MNRAS, 369, 57

Cruz M., Cayon L., Martinez-Gonzalez E., Vielva P., Jin J., 2007, ApJ., 655, 11

de Oliveira-Costa A., Tegmark M., Zaldarriaga M., Hamilton A., 2004, Phys. Rev. D, 69, 063516

Dvorkin C., Peiris H. V., Hu W., 2008, Phys. Rev. D, 77, 063008

Eriksen H. K., Hansen F. K., Banday A. J., Górski K. M., Lilje P. B., 2004, ApJ, 605, 14

Gorski K. M., Hivon E., Banday A. J., Wandelt B. D., Hansen F. K., Reinecke M., Bartelman M., 2005, ApJ, 622, 759

Hajian A., 2007, preprint (astro-ph/0702723)

Hajian A., Souradeep T., 2003, ApJ, 597, L5

Ho S., Hirata C. M., Padmanabhan N., Seljak U., Bahcall N., 2008, Phys. Rev. D, 78, 043519

Huterer D., 2006, New Astron. Rev., 50, 868

Inoue K. T., Silk J., 2006, ApJ, 648, 23

Land K., Magueijo J., 2005a, Phys. Rev. lett., 95, 071301

Land K., Magueijo J., 2005b, MNRAS, 357, 994

McEwen J. D., Vielva P., Hobson M. P., Martinez-Gonzalez E., Lasenby A. N., 2007, MNRAS, 373, 1211

Rudnick L., Brown S., Williams L. R., 2007, ApJ, 671, 40

Schwarz D. J., Starkman G. D., Huterer D., Copi C. J., 2004, Phys. Rev. lett., 93, 221301

Slosar A., Seljak U., 2004, Phys. Rev. D, 70, 083002

Smith K. M., Zahn O., Doré O., 2007, Phys. Rev. D, 76, 043510

Spergel D. N. et al., 2003, ApJS, 148, 175

Spergel D. et al., 2007, ApJS, 170, 377

Tegmark M., de Oliveira-Costa A., Hamilton A. J., 2003, Phys.,Rev., D68, 123523

Vielva P., Martinez-Gonzalez E., Barreiro R. B., Sanz J. L., Cayón L., 2004, ApJ, 609, 22

This paper has been typeset from a TEX/LATEX file prepared by the author.